SPINE RESEARCH

OPEN

# Finite element analysis of a biomimetic artificial cervical intervertebral disc model constructed with 3D lamellar scaffold-strengthened hydrogel

Chang-bo Lu[a], Weichen Dong[b], Xiao-jiang Yang[c], Yun Xue[a], Yang Zhang[b,*], Qiuming Gao[a,*]

**Abstract**

**Background:** Artificial intervertebral discs (AIDs) aim to restore spinal kinematics, but few replicate the natural disc's essential viscoelasticity for shock absorption and stress distribution. The internal mechanics of such biomimetic designs also lack thorough finite element analysis (FEA). Therefore, this study aimed to develop a mechanically biomimetic AID model using a 3D lamellar scaffold-strengthened hydrogel and evaluate its biomechanical performance through integrated experimental testing and FEA.

**Methods:** The biomimetic AID model was evaluated through *in vitro* tests (axial compression, compression shear, axial torsion) and corresponding FEA.

**Results:** Mechanical tests demonstrated a compressive stress–strain curve with a J-shaped profile, with a linear modulus of 10 MPa. The AID exhibited a compression-shear stiffness of 90 $N \cdot mm^{-1}$ and axial torsion stiffness of 0.23 $N \cdot m \cdot degree^{-1}$, with creep behavior comparable to a natural disc. FEA revealed that coherent load transfer through both the interconnections within the lamellar scaffold and the scaffold-hydrogel interface, and the entire AID showed a stress profilometry analogous to natural intervertebral disc.

**Conclusion:** In conclusion, we developed an annulus-nucleus structure biomimetic AID that successfully emulates the viscoelastic and mechanical properties of a natural intervertebral disc, presenting a promising prototype for clinical application.

**Keywords:** biomechanics, biomimetic, cervical disc, finite element analysis, viscoelasticity

## 1. Introduction

The human spine is a marvel of natural engineering, and at its core lies the intervertebral disc (IVD)—a sophisticated structure essential for movement, load-bearing, and shock absorption. This critical component functions as a complex, viscoelastic composite: a soft, hydrated nucleus pulposus (NP) resists compression and distributes pressure, while a tough, collagen-rich annulus fibrosus (AF) provides circumferential strength.[1,2] This synergy creates a system that manages immense mechanical stresses through its fluid dynamics and fibrous architecture.[3,4]

Unfortunately, disc degeneration disrupts this delicate balance, diminishing water content and altering mechanical properties.[4] This breakdown leads to abnormal stress distributions, spinal instability, and pain, underscoring the critical need for effective restoration strategies.[5] While artificial intervertebral discs (AIDs) have been developed to preserve motion, most prevalent designs—such as ball-and-socket or metal–polymer sandwiches—prioritize kinematics over biomechanical fidelity. They often fail to replicate the natural disc's vital viscoelasticity and shock-absorbing functions. Although newer biomimetic designs (e.g., M6, fiber-reinforced hydrogels) show promise in mimicking annulus-nucleus structure and swelling behavior,[6,7] significant gaps remain. Few studies have thoroughly investigated how these viscoelastic AIDs influence stress distribution within the implant and surrounding tissues.[8] Moreover, manufacturing limitations and a lack of sophisticated computer modeling have hindered detailed mechanical analysis.[9,10]

To address these challenges, this study introduces a novel biomimetic AID composed of a 3-dimensional

*C-bL and WD contributed to this article equally.*

[a] Department of Orthopedics, 940th Hospital, Lanzhou, Gansu Province, China, [b] Department of Orthopaedic Surgery, Xijing Hospital, The Air Force Medical University, Xi'an, Shaanxi Province, China, [c] Department of Orthopedics, Nanjing Jinling Hospital, Affiliated Hospital of Medical School, Nanjing University, Nanjing, Jiangsu Province, China.

* Correspondence: Yang Zhang, Department of Orthopedics, Xijing Hospital, the Air Force Medical University, No. 127 Changlexi Road, Xincheng District, Xi'an 710032, China (e-mail: zhangyang@fmmu.edu.cn); Qiuming Gao, Department of Orthopedics, 940th Hospital, Lanzhou 730050, China (e-mail: Gaoqm@sohu.com).



Spine Research (2026) 2:1;37–44

Received: 14 October 2025 / Accepted: 8 February 2026

Published online 23 March 2026

http://dx.doi.org/10.1097/br9.0000000000000030

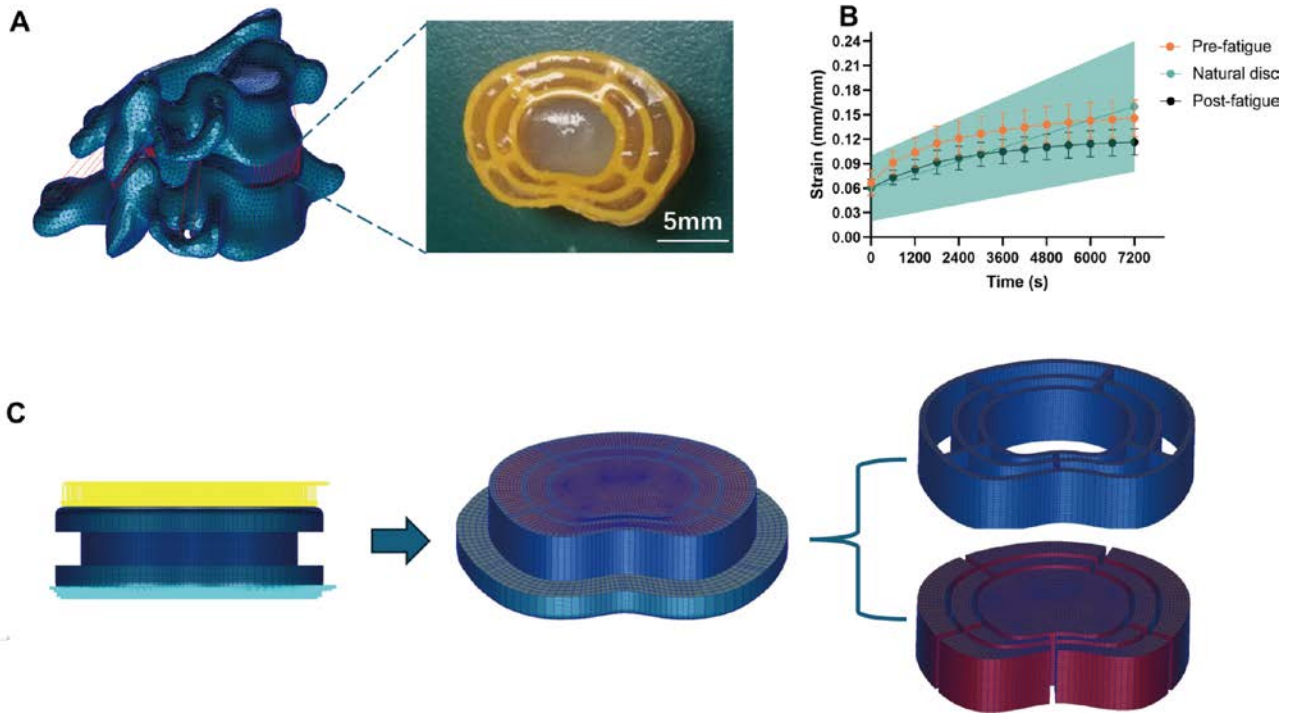


**Figure 1.** Biomimetic AID fabrication, creep behavior, and finite element mesh. (A) AID constructed by the 3D lamellar scaffold-reinforced hydrogel. (B) Compressive creep displacement of the AID for a constant compressive load of 150 N for 2 h before and after dynamic fatigue tests. (C) Finite element mesh of the AID with differentiation of nucleus matrix (purple) and annulus scaffold (blue) regions in the stress-free state, with selected nodes. 3D = 3-dimensional; AID = artificial intervertebral disc.

(3D) lamellar scaffold integrated with an osmotic hydrogel matrix, designed to closely emulate the structure and properties of the natural IVD. Our research aimed to experimentally evaluate the mechanical performance of this prototype under axial compression, shear, and torsion loading and utilize finite element analysis (FEA) to visualize internal stress distributions and validate its biomechanical behavior. By bridging the gap between biomimetic design and rigorous mechanical evaluation, this work offers a meaningful step toward the development of AIDs that not only restore motion but also truly recapitulate the spine's natural biomechanics.

## 2. Materials and methods

### 2.1. Fabrication of the biomimetic AID

A biomimetic AID was designed based on the dimensions and multilamellar structure of the human C6–C7 disc. A 3D lamellar scaffold, representing the AF, was fabricated using a fused deposition modeling machine and medical-grade thermoplastic polyurethane (TPU; Tecoflex® LM-63D; Lubrizol, Cleveland, Ohio) with a tensile modulus of 23–33 MPa. The NP was simulated using a polyacrylamide hydrogel. A pregel solution was prepared by mixing 10 wt% acrylamide (A8887; Sigma, Saint Louis), 10 wt% *N*,*N*-methylenebisacrylamide (146072; Sigma) as a crosslinker, and 0.1 wt% ammonium persulphate (248614; Sigma) as a photoinitiator. The solution was degassed in a vacuum chamber, after which 40 wt% nano-$Al_2O_3$ (702129-100G; Sigma) was added as a crosslinking accelerator. The flexible TPU scaffold was then placed in a mold, and the pregel solution was poured and infused into it. The assembled AID was ultraviolet-cured for 30 min and stored in a humid box for 24 h to allow the reaction to stabilize. The final AID had nominal lateral and sagittal diameters of 25 and 18 mm, respectively, and a nominal height of 7 mm under preload (Fig. 1A).

### 2.2. Mechanical testing

Fifteen AID samples were fabricated for mechanical characterization. Creep tests were conducted on a material testing system (ElectroUniversal Testing Machine, AGS-X-300kN; SHIMADZU, Tokyo, Japan) in a 0.15 M NaCl bath maintained at 37 °C.

***2.2.1. Axial compression, compression shear, and axial torsion (Fig. 2A–C).*** Samples were mounted between custom stainless steel fixtures (conforming to standard F2346-05) to simulate a spinal motion segment. Axial compression tests were performed at a strain rate of 5 mm·min$^{-1}$ up to a load of 2 kN. Failure was defined as a force drop of > 5% at constant displacement or a thickness reduction of > 50% compared with the postpreconditioning thickness. Strength was defined as the peak load before failure. Compression-shear testing was initiated with the device's *Z*-axis rotated +45° about the *Y*-axis. For torsion tests, a combined compressive force (*F*) and moment (*M*) were applied, with bending moment minimized.

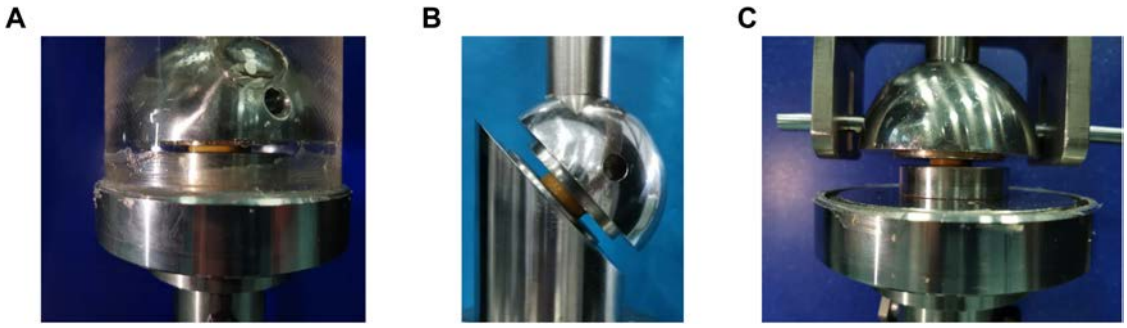


**Figure 2.** Test facilities for performing mechanical tests of the artificial intervertebral disc model. (A) The quasi-static compressive test facility with a Dynacell loadcell of 10 kN capacity. (B) The quasi-static compressive-shear test facility. (C) The quasi-static compressive-torsion test facility.

***2.2.2. Dynamic fatigue test.*** In the fatigue tests, the AIDs were axially loaded (150–1500 N) at 5 Hz. A diurnal cycle, consisting of 16-h loading and 8-h recovery at 50 N. "Failure" was defined as 1 or more of the following[10]: a decrease (> 20%) in thickness compared with the beginning of the loading period; a thickness decrease (> 5%) at the start of 1 loading period relative to the previous one; a thickness decrease (> 50%) compared with the thickness after preconditioning; or visible extrusion of gel particles.

***2.2.3. Compressive creep.*** Before and after fatigue tests, a compressive creep test was carried out. An axial load of 150 N was applied for 7200 s (2 h) in a saline bath at 37 ± 0.5 °C, and strain was monitored. The constant load of 150 N was applied using a linear ramp loading regime for 5 s as described previously.[11] The last creep curve was compared with the range of natural IVD responses, as described by the creep model used by Skrzypiec et al.[12]

### *2.3. Finite element analysis*

***2.3.1. Model development.*** Finite element models of the AID and its clamping apparatus were reconstructed using 3D reverse engineering technology in Geomagic Studio 2014 software to simulate an *in vivo* motion segment. The model, consisting of the biomimetic disc and fixtures, was meshed with 273,436 nodes and 263,500 IsoMesh Hex8 elements. A binding contact was defined between structural grids to ensure uninterrupted stress transmission. The meshed model was processed using Hypermesh 13.0 software (Fig. 1).

Mesh sensitivity analysis was performed by refining the mesh from approximately 120,000 to 400,000 elements. The results for peak stress in the annulus and nucleus changed by less than 3% between the medium (about 260,000 elements) and fine meshes, confirming that the chosen mesh density provided converged and reliable results.

***2.3.2. Material properties.*** The bone tissue of the vertebrae, endplates, and the interspinous cartilage was described by isotropic and linear-elastic material properties.[13–15] Material properties were assigned based on literature values and measured data (Table 1). Vertebral bone, endplates, and cartilage were modeled as isotropic, linear-elastic materials. The AID's AF was modeled as a hydrogel matrix reinforced with 3 concentric TPU layers, assigned an isotropic, linear-elastic modulus of 20 MPa in the circumferential direction.[14,16,17] The NP was modeled as an isotropic, viscoelastic hydrogel with a compressive modulus of 0.5 MPa. Articulating surfaces used surface-to-surface contact elements (penalty algorithm, friction coefficient = 0.1), mirroring natural disc kinematics.[18,19] The penalty stiffness was tuned to minimize penetration while maintaining numerical stability. The stainless steel (SS304) clamping apparatus was assigned an elastic modulus of 195 GPa and a Poisson's ratio of 0.247.

***2.3.3. Boundary and loading conditions.*** Simulations replicated the 3 experimental mechanical tests: axial compression, compression shear, and axial torsion. A compression preload of 150 N was applied in all stages.[20,21] Subsequently, for compression shear, a 150 N shear force was applied; for torsion, a 6° rotational motion was applied. In all simulations, the load was applied to the superior fixture, while all 6° of freedom were constrained for the nodes on the inferior fixture surface.

### *2.4. Statistical analysis*

For all material parameters, statistical differences were determined with a one-way analysis of variance. For creep duration analysis, the Bonferroni pairwise comparison was applied.

## 3. Results

### *3.1. Mechanical properties*

The AID samples did not fail under compressive loads up to 2 kN (corresponding to 50%–60% strain). The stress–strain curve exhibited a J-shaped profile, with a toe region extending to about 10% strain, followed by a linear region. The compressive modulus, derived from the linear region, was 10.0 MPa at a strain rate of

**Table 1**

**Material properties in the FE analysis.**

| Structure | Materials | Elastic modulus (MPa) | Poisson's ratio |
|---|---|---|---|
| Annulus fibrosus scaffold | TPU | 20 | 0.31 |
| Nucleus pulposus matrix | Hydrogel | 0.5 | 0.499 |
| Clamping apparatus | Stainless steel (SS304) | 195,000 | 0.247 |

FE = finite element; TPU = thermoplastic polyurethane.

5 mm·min$^{-1}$ (Fig. 3A). The compression–shear stiffness was 90 N·mm$^{-1}$ (Fig. 4A), and the torsional stiffness was 0.23 N·m·degree$^{-1}$ (Fig. 5A). To evaluate the viscoelasticity, the time-dependent creep tests were conducted. Under a constant axial load at 150 N, the prosthesis exhibited viscoelastic strain values ranging from 6.1% to 14.6% over 2 h, demonstrating a trend of progressively decelerating deformation. The creep strain of the postfatigue artificial IVDs is lower (the difference is not statistically significant), ranging from 4.9% to 11.7%. Both prefatigue and postfatigue creep strain values fall within the natural disc range (Fig. 1B). Such a curve aligned well with the response range reported for natural cervical IVDs under similar loading (Fig. 1A).[12]

### 3.2. Finite element analysis

Finite element analysis was employed to quantify internal stress distributions and biomechanical behavior under load, specifically measuring layer height (*H*) changes and bulging in the AF.

### 3.3. Axial compression (Fig. 3)

The superior surface of the AID sustained an average stress of 1.64 MPa (peak: 2.31 MPa), while the inferior surface bore 0.38 MPa (peak: 0.84 MPa) (Fig. 3E and F). The reinforcing fiber layer sustained a radial stress of 1.67 MPa, and the hydrogel NP core bore a stress of 0.78 MPa. The artificial disc exhibited a radially decreasing stress profile, which was primarily localized within the inner scaffold. The lamellar scaffold effectively restricted the hydrogel matrix from horizontal buckling.

### 3.4. Compression shear (Fig. 4)

Under shear loading, the superior surface sustained an average stress of 0.22 MPa (peak: 0.38 MPa), and the inferior surface bore 0.13 MPa (peak: 0.26 MPa) (Fig. 4E and F). The fiber layer and NP bore radial stresses of 0.44 and 0.39 MPa, respectively. The fixture connection minimized stress concentration.

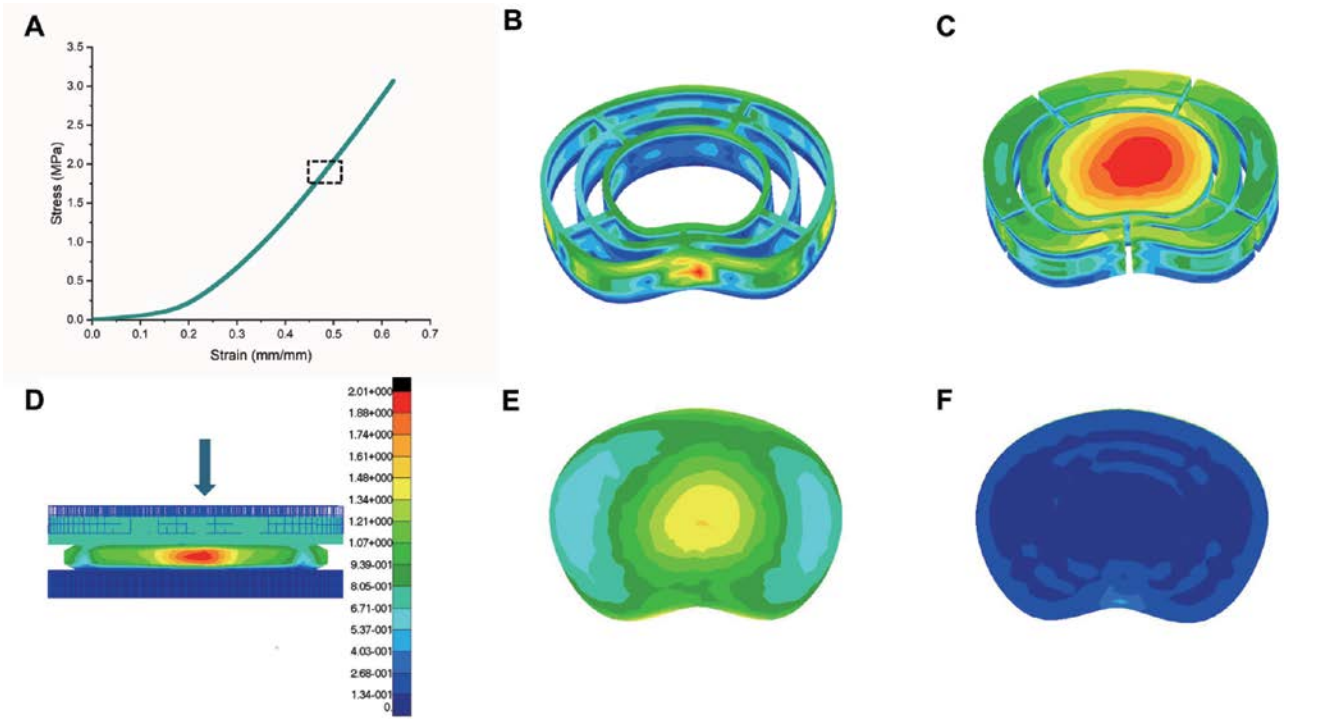


**Figure 3.** Mechanical response and stress distribution of the AID under axial compression. (A) Compressive stress–strain curves of the AID at a strain rate of 5 mm/min. (B) The stress profilometry across the 3D lamellar scaffold of the AID in axial compression. (C) The stress profilometry across the hydrogel matrix of the AID in axial compression. (D) Color plot of an axially compression-loaded model with 150 N at 60 s. (E) The stress profilometry across the superior surface of the AID in axial compression. (F) The stress profilometry across the inferior surface surface of the AID in axial compression. 3D = 3-dimensional; AID = artificial intervertebral disc.

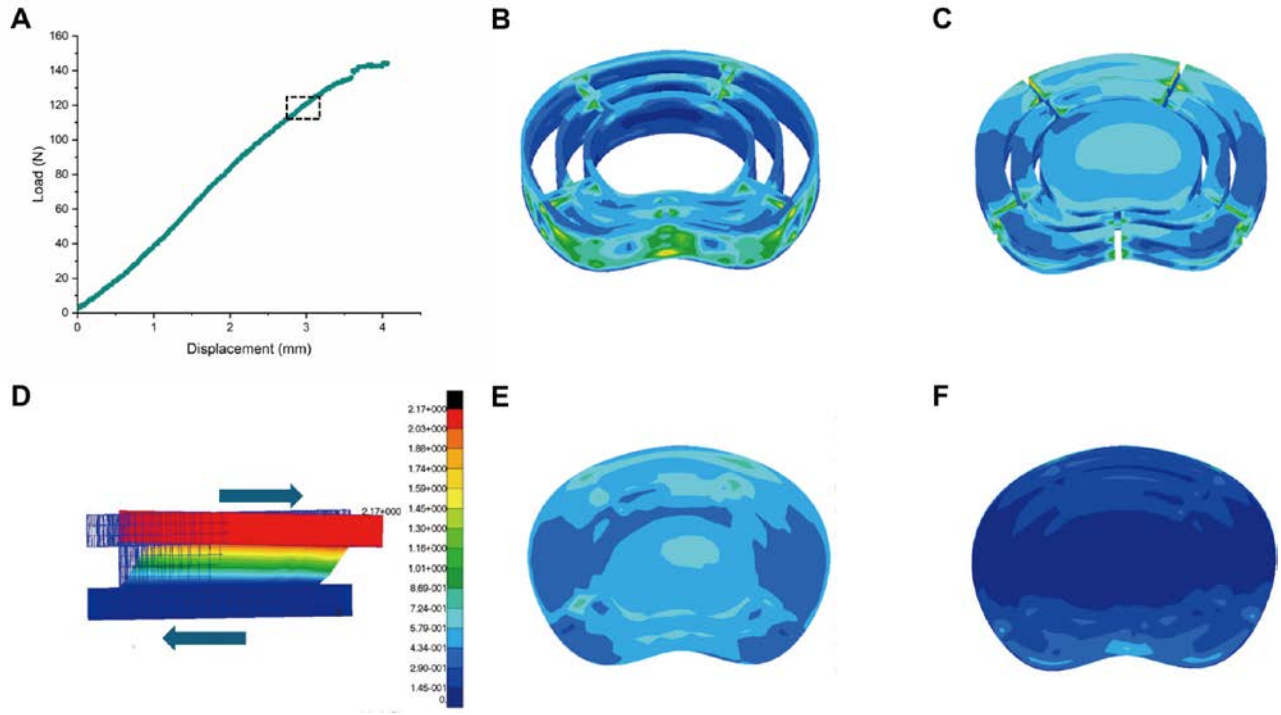


**Figure 4.** Mechanical response and stress distribution of the AID under compression-shear loading. (A) Compressive load–displacement curves of the AID at a strain rate of 5 mm/min. (B) The stress profilometry across the 3D lamellar scaffold of the AID in compression shear. (C) The stress profilometry across the hydrogel matrix of the AID in compression shear. (D) Color plot of an axial compression shear-loaded model with 150 N at 60 s. (E) The stress profilometry across the superior surface of the AID in compression shear. (F) The stress profilometry across the inferior surface of the AID in compression shear. 3D = 3-dimensional; AID = artificial intervertebral disc.

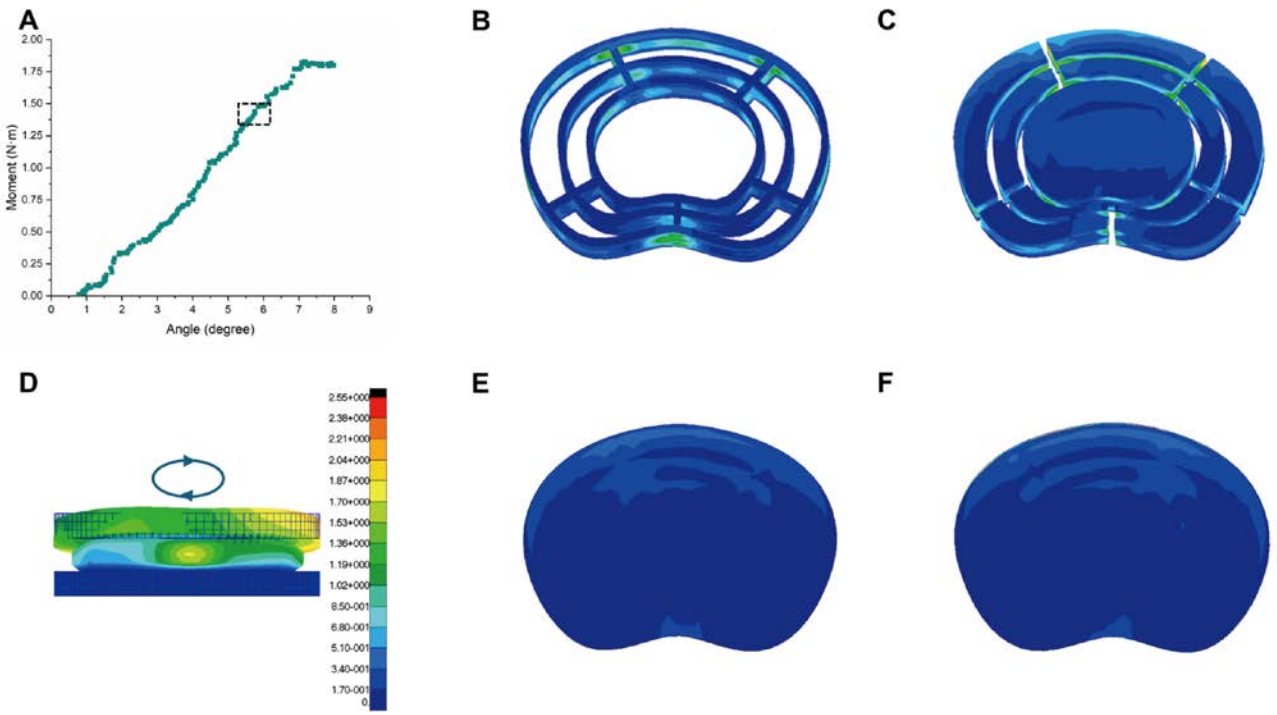


**Figure 5.** Mechanical response and stress distribution of the AID under axial torsion. (A) Axial rotation moment–degree curves of the AID in position control at a rate of 6°/min. (B) The stress profilometry across the 3D lamellar scaffold of the AID in axial rotation. (C) The stress profilometry across the hydrogel matrix of the AID in axial rotation. (D) Color plot of an axially torsion-loaded model with a rotation angle of 6° at 60 s. (E) The stress profilometry across the superior surface of the AID in axial rotation. (F) The stress profilometry across the inferior surface of the AID in axial rotation. 3D = 3-dimensional; AID = artificial intervertebral disc.

### 3.5. Axial torsion (Fig. 5)

In the axial torsion test, the superior surface sustained an average stress of 0.35 MPa (peak: 0.84 MPa), and the inferior surface bore 0.32 MPa (peak: 0.77 MPa) (Fig. 5E and F). The fiber layer and NP bore the highest stresses at 1.90 and 0.93 MPa, respectively. The fixture was displaced by 1.52 mm, but prevented excessive buckling.

### 3.6. Stress profile of the macroscale disc model

Figure 6A–C correlates the stress contour plot with the regional stress distribution in the AID under different loading conditions. A ripple-shaped contour can be observed for all normal stress components. The magnitude of transverse normal components increases consistently when approaching to the NP, which is considered to be caused by the radial constraint from the lamellar AF. The stiffness of NP hydrogel is much lower than that of AF. When the axial compression load is applied, the composite ring is barely stretched, thus causing less constraint onto the hydrogel core. While under the compression shear or axial torsion load, the lamellar scaffold is stretched. In this case, the stress magnitude concentrated at the annulus fibrosis, indicating the critical constraint at the radial direction, as illustrated in Figure 6D. A ring of stress concentration along the interfacial region can also be seen, and it appears more conspicuous as the overall strain increases.

## 4. Discussion

The development of AIDs has historically progressed slowly, one of the challenges primarily attributed to the complex physiological and biomechanical nature of the native disc.[22] Clinical adoption has been limited by issues such as particulate wear debris and a fundamental mismatch in mechanical properties between existing prostheses and the natural IVD, often leading to adjacent segment degeneration. In response to this need, our study presents a novel biomimetic AID prototype that integrates a 3D-printed TPU lamellar scaffold—mimicking the AF—with a viscoelastic polyacrylamide hydrogel nucleus. This design philosophy is grounded in the understanding that the natural IVD is a fiber-reinforced, lamellar, and viscoelastic composite structure. Our results demonstrate that this composite model successfully replicates the key biomechanical and viscoelastic properties of the human cervical disc.

A significant hurdle in AID design is that synthetic hydrogels, while biocompatible and hydrous, are often mechanically compliant and fragile compared with the tough, resilient native tissue.[23,24] The prevailing principle for creating tough hydrogel systems involves incorporating mechanisms for efficient energy dissipation while retaining high elasticity.[25] Our design addresses this by utilizing the 3D-printed TPU scaffold to provide high tensile strength and structural integrity, while the hydrogel matrix contributes energy dissipation through its viscoelastic behavior. This synergistic interaction was evident in the characteristic J-shaped stress–strain curve

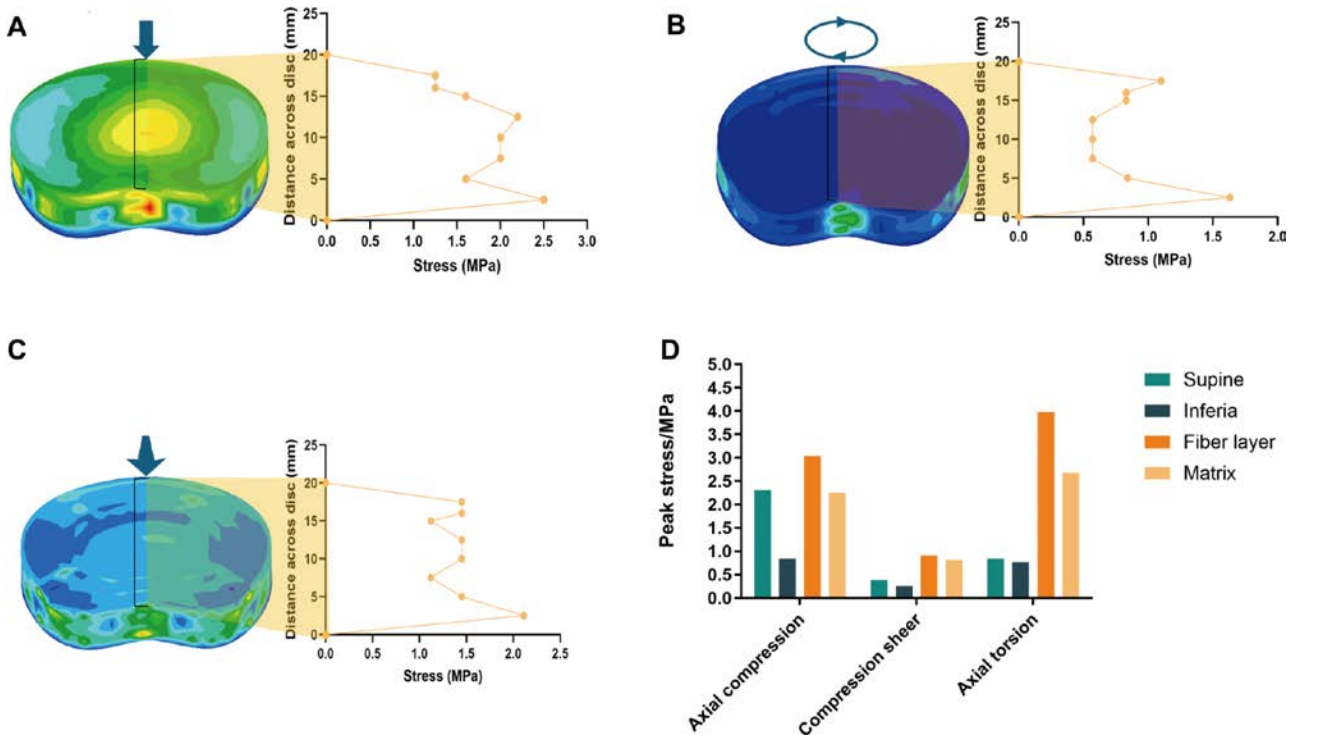


**Figure 6.** Regional stress distribution across the AID under different loading conditions. (A–C) The stress profile map across the disc model under compression, compressive-shear, and compressive-torsion loading. (D) The peak stress values of different parts of the AID structures in FE analysis. AID = artificial intervertebral disc; FE = finite element.

under axial compression, a hallmark of natural soft tissues. The initial toe region represents the uncrimping and alignment of collagen fibers in the natural annulus, which in our model is replicated by the gradual engagement of the reinforcing scaffold fibers. The subsequent linear region reflects the dominant elastic response of these straightened fibers. Furthermore, the prosthesis exhibited compression shear and axial torsion stiffness values (90 $N \cdot mm^{-1}$ and 0.23 $N \cdot m \cdot degree^{-1}$, respectively) that satisfy the basic mechanical requisites for cervical disc replacement. Crucially, the time-dependent creep behavior of our AID closely approximated that of natural cervical IVDs, underscoring its capacity for critical shock-absorbing functions. It is noteworthy that the artificial IVD remained intact and free from delamination after periodic 5 million fatigue loading. Although the AIDs did become stiffer in the loading process, with a decrease in creep strain (Fig. 1B). Nevertheless, the mechanical property values remained within the reference ranges of its natural counterpart. The excellent durability of the AID can be attributed to the tough and self-healable hydrogel, which automatically repairs in response to damage.

Our work advances the field beyond previous biomimetic efforts. For instance, van den Broek et al.[10] developed a promising prototype with a hydrogel core and fiber encapsulation. However, its manual fabrication introduced structural inconsistencies that precluded reliable FEA and precise customization. Gullbrand et al.[1] developed a layered scaffold consisting of 3 different components to mimic natural spinal motion segments. In our previous work, we applied linear motors to weave glass fibers into a scaffold structure and then injected a self-healing, tough nanocomposite hydrogel.[26] This scaffold, made of 3D braided fibrous textiles and a hydrogel, mimicked the 3D tetragonal fibrous structures of natural AF and natural NP, respectively. FEA of the artificial IVD from mesoscale and macroscale analysis indicates the coherent load transfer through both the interconnections within the fiber mesh and the fiber–matrix interface. In contrast to the complex structures, we developed a simplified lamellar scaffold–matrix compsite to elucidate and verify the underlying mechanical significance of native annulus-nucleus structure. In addition, our use of computer-aided design and 3D printing ensures high reproducibility, allows for patient-specific customization of structural parameters (e.g., lamellar spacing and fiber orientation), and facilitates direct integration with computational modeling. This represents a significant methodological improvement for the iterative design and analysis of AIDs.

The FEA results provide critical insight into the internal mechanical environment of our AID, a feature difficult to assess experimentally. The model revealed a stress distribution pattern consistent with findings in natural IVDs, where the highest compressive stresses are concentrated in the hydrostatic NP, and stress within the annulus decreases radially outwards.[19,27] This validates the biomimetic performance of our design. However, the analysis also indicated that the average and peak stress values under load were higher than those reported in some cadaveric studies. This discrepancy may be attributed to 2 factors: the application of a 150 N load, which represents an upper-limit scenario (e.g., head-helmet system) rather than pure physiological loading; and the absence of posterior spinal elements (facet joints, ligaments) in our isolated segment model. In an intact spine, these posterior structures share a significant portion (up to 64%) of the axial load, thereby reducing the stress borne by the disc itself.

## 5. Limitations

Despite promising results, this study has several limitations. First, the *in vitro* model lacked surrounding musculoskeletal structures, which are essential for replicating the full *in vivo* loading environment. Future work should incorporate these elements into more complex FEA models and utilize spinal motion simulators for experimental validation. Then, the current analysis focused on short-term mechanical performance. Long-term fatigue testing, wear analysis of the hydrogel–scaffold interface, and comprehensive biocompatibility assessments are essential next steps to evaluate the implant's durability and safety. In addition, the fully fixed boundary condition of the lower fixture, while matching the experimental setup, may introduce higher interfacial stresses compared with the compliant support of vertebral bone *in vivo*. Finally, while the material properties were based on literature values, further characterization of the hydrogel's permeability and the scaffold's anisotropic properties could refine the FEA models. Future studies should also incorporate multisegment spinal models with realistic vertebral mobility and posterior elements (facet joints and ligaments) to evaluate coupled motions and load-sharing across adjacent levels, providing a more comprehensive simulation of the *in vivo* biomechanical environment.

## 6. Conclusion

In conclusion, to our knowledge, this study is the first to integrally combine experimental biomechanical testing with detailed FEA of the internal mechanical state in a fully biomimetic, 3D-printed AID. Our prototype, characterized by its annulus-nucleus structure, successfully emulates the viscoelastic, shock-absorbing, and load-bearing capabilities of the natural cervical disc. This work not only provides a feasible design paradigm for a new generation of AIDs but also establishes a robust framework for their computational evaluation and iterative optimization, paving the way for more successful clinical applications in the future.

## Acknowledgements

Xiaojiang Yang discloses support for the research of this work from National Natural Science Foundation of China [82302773].

## Ethical statement

This article does not contain any studies with human participants or animals performed by any of the authors.

## Conflicts of interest

The authors have no conflicts of interest to disclose.

## Funding source

XY discloses support for the research of this work from the National Natural Science Foundation of China (82302773).

## Data availability statement

The datasets used and/or analyzed during the current study are available from the corresponding author on reasonable request.

## Author contributions

[Yang Zhang, Qiu-ming Gao] : Conceptualization. [Changbo Lu, Wei-chen Dong]: Methodology, Writing – Original Draft. [Changbo Lu, Xiaojiang Yang] : Software, Validation, Investigation. [Wei-chen Dong Xiao-jiang Yang] : Formal Analysis, Data Curation. [Qiu-ming Gao and Yang Zhang] : Writing – Review & Editing, Supervision. All authors reviewed and approved the final manuscript.

## References

[1] Gullbrand SE, Ashinsky BG, Bonnevie ED, et al. Long-term mechanical function and integration of an implanted tissue-engineered intervertebral disc. *Sci Transl Med*. 2018;10:eaau0670.
[2] Sun Z, Sun Y, Lu T, Li J, Mi C. A swelling-based biphasic analysis on the quasi-static biomechanical behaviors of healthy and degenerative intervertebral discs. *Comput Methods Programs Biomed*. 2023;235:107513.
[3] Frazer LL, Shaffer SK, Seifert J, Stemper BD, Nicolella DP. Modeling fatigue and damage development in the annulus fibrosus using a reactive viscoelastic framework. *Ann Biomed Eng*. 2026.
[4] Sciortino V, Jansen JU, Cerniglia D, Ingrassia T, Wilke H-J. Intervertebral disc creep behaviour through viscoelastic models: an *in-vitro* study. *Discov Appl Sci*. 2024;6:392.
[5] Feki F, Taktak R, Haddar N, Moulart M, Zaïri F, Zaïri F. Overloading effect on the osmo-viscoelastic and recovery behavior of the intervertebral disc. *Proc Inst Mech Eng H*. 2024;238:430–7.
[6] Shikinami Y, Kawabe Y, Yasukawa K, Tsuta K, Kotani Y, Abumi K. A biomimetic artificial intervertebral disc system composed of a cubic three-dimensional fabric. *Spine J*. 2010;10:141–52.
[7] Gloria A, Causa F, De Santis R, Netti PA, Ambrosio L. Dynamic-mechanical properties of a novel composite intervertebral disc prosthesis. *J Mater Sci Mater Med*. 2007;18:2159–65.
[8] Nasiri Y, Khosravifard A. Investigating the effects of geometrical parameters of an artificial cervical disc in vulnerable neck positions on the stress distribution in the spine using 3D finite element analysis. *Proc Inst Mech Eng H*. 2025;239:624–35.
[9] Van den Broek PR, Huyghe JM, Wilson W, Ito K. Design of next generation total disk replacements. *J Biomech*. 2012;45:134–40.
[10] van den Broek PR, Huyghe JM, Ito K. Biomechanical behavior of a biomimetic artificial intervertebral disc. *Spine*. 2012;37:E367–73.
[11] Skrzypiec DM. *Mechanical Functioning of Human Cervical Intervertebral Discs*. University of Bristol; 2006.
[12] Skrzypiec D, Pollintine P, Przybyla A, Adams M. Creep behaviour of human cervical intervertebral discs. Paper/Poster presented at: Orthopaedic Proceedings; July 1, 2008. 2008.
[13] Shirazi-Adl SA, Shrivastava SC, Ahmed AM. Stress analysis of the lumbar disc-body unit in compression a three-dimensional nonlinear finite element study. *Spine*. 1984;9:120–34.
[14] Zahaf S, Habib H, Mansouri B, Belarbi A, Azari Z. The effect of the eccentric loading on the components of the spine. *Hematol Med Oncol*. 2016;1:1–10.
[15] Kim H-J, Kang K-T, Chang B-S, Lee C-K, Kim J-W, Yeom JS. Biomechanical analysis of fusion segment rigidity upon stress at both the fusion and adjacent segments: a comparison between unilateral and bilateral pedicle screw fixation. *Yonsei Med J*. 2014;55:1386–94.
[16] Dong RC, Guo LX. Human body modeling method to simulate the biodynamic characteristics of spine *in vivo* with different sitting postures. *Int J Numer Method Biomed Eng*. 2017;33:e2876.
[17] López E, Ibarz E, Herrera A, et al. Probability of osteoporotic vertebral fractures assessment based on DXA measurements and finite element simulation. *Adv Biosci Biotechnol*. 2014;05:527–45.
[18] Biswas JK, Malas A, Majumdar S, Rana M. A comparative finite element analysis of artificial intervertebral disc replacement and pedicle screw fixation of the lumbar spine. *Comput Methods Biomech Biomed Engin*. 2022;25:1812–20.
[19] Leszczynski A, Meyer F, Charles Y-P, Deck C, Willinger R. Development of a flexible instrumented lumbar spine finite element model and comparison with *in-vitro* experiments. *Comput Methods Biomech Biomed Engin*. 2022;25:221–37.
[20] Yoganandan N, Umale S, Stemper B, Snyder B. Fatigue responses of the human cervical spine intervertebral discs. *J Mech Behav Biomed Mater*. 2017;69:30–8.
[21] Skrzypiec DM, Pollintine P, Przybyla A, Dolan P, Adams MA. The internal mechanical properties of cervical intervertebral discs as revealed by stress profilometry. *Eur Spine J*. 2007;16:1701–9.
[22] Khanna A, Jain P, Paul CP. Towards biomimetic evolution of artificial intervertebral disc: a review. *Med Biol Eng Comput*. 2025;63:2853–69.
[23] Desai SU, Srinivasan SS, Kumbar SG, Moss IL. Hydrogel-based strategies for intervertebral disc regeneration: advances, challenges and clinical prospects. *Gels*. 2024;10:62.
[24] Beall DP, Amirdelfan K, Nunley PD, Phillips TR, Imaz Navarro LC, Spath A. Hydrogel augmentation of the lumbar intervertebral disc: an early feasibility study of a treatment for discogenic low back pain. *J Vasc Interv Radiol*. 2024;35:51–8.e1.
[25] Li X, Gong JP. Design principles for strong and tough hydrogels. *Nat Rev Mater*. 2024;9(6):380–98.
[26] Lu C, Huang X, Yan H, et al. Biomimetic design of 3D fibrous mesh reinforced hydrogel replicating the form and function of the intervertebral disc. *Small Struct*. 2023;4:2200254.
[27] Ansaripour H, Ferguson SJ, Flohr M. *In vitro* biomechanics of the cervical spine: a systematic review. *J Biomech Eng*. 2022;144:100801.

How to cite this article: Lu C-B, Dong W, Yang X-J, Xue Y, Zhang Y, Gao Q. Finite element analysis of a biomimetic artificial cervical intervertebral disc model constructed with 3D lamellar scaffold-strengthened hydrogel. *Spine Res*. 2026;2(1):e00030. doi: 10.1097/br9.0000000000000030